THEORETICA CHIMICA ACTA

Theoret. Chim. Acta (Berl.) 63, 401–419 (1983)

Ab initio and Model Hypersurfaces for Ground and Excited State Radical Reactions

Udo Höweler and Martin Klessinger

Organisch-Chemisches Institut der Universität Münster, Orléans-Ring 23, D-4400 Münster, Federal Republic of Germany

A graphical representation of the potential energy hypersurfaces of the three-centre three-electron problem is proposed which is sufficient to fully describe the system. This method is used to visualize the hypersurfaces of the ground and the first excited doublet state of H_3, obtained from VBCI calculations as well as from a judiciously parametrized HMO model and a semiempirical HL model. On the basis of these results three prototype radical reactions are discussed and the performance of the semiempirical models is assessed by comparison with the *ab initio* results, in order to see which features of the models are essential for a correct description of radical reactions. The importance of overlap within the MO approach and of electron interaction within the semiempirical HL method is thus revealed.

Key words: Graphical representation of potential hypersurfaces – MO and HL models – Radical reactions – Three-centre three-electron system – VB calculations.

1. Introduction

Potential hypersurfaces of ground and excited states of the three-centre three-electron problem may be of interest for a number of reasons. First, they may be viewed as model surfaces for thermal and photochemical free radical reactions, in particular of free radical addition to or substitution on closed-shell systems and intramolecular rearrangements, second, they form an example of hypersurfaces simple enough to be fully treated and therefore, they help to study methodological problems of suitable pictorial representation and of information retrieval from multidimensional surfaces. Finally, they can be used to test and compare the performance of MO and VB methods.

The simplest three-centre three-electron system is H_3 which has been the subject of numerous theoretical and experimental investigations, which have been reviewed extensively [1]. Recent papers [2] are mainly concerned with Rydberg states of H_3 which were first observed experimentally by Herzberg [3]. Accurate calculations were published by Shavitt et al. [4] and by Liu et al. [5] and an excellent least square fit to the ground state surface of Ref. [5] was given by Truhlar and Horowitz [6]. Van der Waals minima in the ground state were treated by Tennyson [7]; Zaitsevskii et al. [8] and Wu [9] calculated the ground and lower excited states on the basis of Diatomics in Molecules. The conditions for semiempirical MO methods to predict correctly the instability of H_3 were discussed by Calzaferri [10]. More general descriptions of the three-centre three-electron system and free radical reactions were given by Yamaguchi et al. [11] on the basis of spin symmetry and by Bonačič-Koutecký et al. [12] using simple MO and VB treatments.

In the present paper, we use the same models to discuss the ground state as well as the first excited state of the three-centre three-electron problem. In addition, non-empirical VB calculations are performed on these two states of H_3 in order to check the validity of the semiempirical models and to find out, to what extent generalizations are possible for free radical reactions of larger systems. In the case of H_4 Gerhartz et al. [13] used a similar approach to discuss the ground state and photochemical reactivity of the closed-shell four-centre four-electron problem.

2. Theoretical Methods

The Hückel-MO-model (HMO), which leads to uncorrelated wave functions, and the Heitler–London Valence Bond (HL) model, which overemphasizes correlation, represent two opposite extremes for the theoretical discussion of electronic structures. By interpolation between these two models it should be possible to explore the essential features of a chemical system or a chemical reaction [14].

Within the HMO model without overlap the secular equation of the three-centre three-electron system may be written as:

$$-x^3+(B_{12}^2+B_{13}^2+B_{23}^2)x+2B_{12}B_{13}B_{23}=0 \tag{1}$$

where the variables are defined as

$$-x=\frac{\alpha-\varepsilon}{\beta_0} \quad \text{and} \quad B_{\mu\nu}=\frac{\beta_{\mu\nu}}{\beta_0},$$

using the resonance integral β_0 as reference and energy unit.

From the solutions of Eq. (1) and the assumption of constant α's the binding energies of the ground configuration and first excited configuration are

$$E_0^B=2\varepsilon_1+\varepsilon_2-3\alpha \qquad E_1^B=2\varepsilon_1+\varepsilon_3-3\alpha. \tag{2}$$

Usually the parameters $B_{\mu\nu}$ are set equal to 1 for bonded centres μ and ν and zero otherwise. If this is done, the following results are obtained for the special cases, which correspond to a Z_2 and a distant Z (Z_2+Z), to linear Z_3 (Z_3 lin) and an equilateral Z_3 (Z_3 cyc), respectively:

$$\begin{aligned}
&B_{12}=1, \quad B_{13}=B_{23}=0 && E_0^B(Z_2+Z)=2\beta_0 && E_1^B(Z_2+Z)=1\beta_0\\
&B_{12}=B_{23}=1, \quad B_{13}=0 && E_0^B(Z_3\,\text{lin})=2\cdot\sqrt{2}\beta_0 && E_1^B(Z_3\,\text{lin})=\sqrt{2}\beta_0\\
&B_{12}=B_{23}=B_{13}=1 && E_0^B(Z_3\,\text{cyc})=3\beta_0 && E_1^B(Z_3\,\text{cyc})=3\beta_0.
\end{aligned} \tag{3}$$

Thus an increasing stabilization of the ground state configuration is observed in going from the separated system to the system with equal distances between the centres 1, 2 and 2, 3 respectively ($D_{\infty h}$ symmetry) and finally to the D_{3h} geometry, where the ground and excited configurations are degenerate.

In order to describe different geometries more flexibly, values other than 1 and 0 should be allowed for $B_{\mu\nu}$; we use the following parametrization: the resonance integrals β are set proportional to the overlap integrals between 1s orbitals with corresponding bond distance, and the $B_{\mu\nu}$ values were obtained by using the β parameter for the linear H_3 system as a reference β_0. Within this parametrization the B_{12} value for the bonded atoms of the Z_2+Z system is 1.5, therefore $E_0^B(Z_2+Z)$ is equal to $3\beta_0$ and the energetical ordering of the Z_2+Z and linear Z_3 arrangements is reversed.

The qualitative HL model is more difficult to parametrize. We follow the suggestions of Bonačić-Koutecký et al. [12] and write the secular determinant for the interaction of the two doublet functions

$$\begin{aligned}
{}^2\Psi_1 &= \frac{1}{\sqrt{2}}\{|\chi_1\bar{\chi}_2\chi_3|-|\bar{\chi}_1\chi_2\chi_3|\}\\
{}^2\Psi_2 &= \frac{1}{\sqrt{6}}\{2|\chi_1\chi_2\bar{\chi}_3|-|\chi_1\bar{\chi}_2\chi_3|-|\bar{\chi}_1\chi_2\chi_3|\}
\end{aligned} \tag{4}$$

in the form

$$\begin{vmatrix}
A-I+\mathcal{J}_{12}-\tfrac{1}{2}(\mathcal{J}_{23}+\mathcal{J}_{13})-E(1-\mathcal{S}+\sigma_1) & \frac{\sqrt{3}}{2}(\mathcal{J}_{23}-\mathcal{J}_{13})-E\sigma_2\\
\frac{\sqrt{3}}{2}(\mathcal{J}_{23}-\mathcal{J}_{13})-E\sigma_2 & A-I-\mathcal{J}_{12}+\tfrac{1}{2}(\mathcal{J}_{23}+\mathcal{J}_{13})-E(1-\mathcal{S}-\sigma_1)
\end{vmatrix} \tag{5}$$

with

$$\begin{aligned}
A &= \sum_i h_{ii}+\sum_{i<j}(ii|jj)+\sum_{A<B}\frac{Z_AZ_B}{R_{AB}}\\
I &= h_{ij}S_{ik}S_{kj}+S_{kj}(ki|ij)+\text{cycl. permutations}\\
\mathcal{J}_{ij} &= S_{ij}[2h_{ij}+S_{ij}h_{kk}+2(ij|kk)]+(ij|ji)\\
\mathcal{S} &= S_{12}S_{13}S_{23}\\
\sigma_1 &= \tfrac{1}{2}[2S_{12}^2-S_{13}^2-S_{23}^2], \quad \sigma_2=S_{23}^2-S_{13}^2.
\end{aligned} \tag{6}$$

As Epiotis suggested [15], quantities of these types can be interpreted in the following way: A contains all the "classical" terms, and since the nucleus–electron Coulomb interactions contained in the one-electron AO energies h_{ii} and the electron–electron and nucleus–nucleus Coulomb interactions approximately cancel each other, A can be assumed to be constant. I consists of "semiclassical" terms which are proportional to the third order of the overlap integrals and contain three-centre integrals. Therefore, they should come into play only for short internuclear distances.

The "non-classical" valence bond exchange integrals $\mathcal{J}_{ij}$ are larger than I and being approximately proportional to the square of the overlap integrals, they can be used to describe different geometrical arrangements of the Z_3 system.

If one neglects $\mathcal{S}$, being third order in the overlap integrals, and σ, consisting of the differences of the squares of overlap integrals, the relative HL energies may be written as

$$E^B_{0,1} = \pm \frac{|\mathcal{J}_0|}{\sqrt{2}} [(J_{12}-J_{13})^2 + (J_{12}-J_{23})^2 + (J_{13}-J_{23})^2]^{1/2} \tag{7}$$

(cf. [16]). The energies of the covalent ground and excited states are symmetrical with respect to A–I, which is taken as zero and $\mathcal{J}_0$ is taken as a reference exchange integral to define $J_{ij} = \mathcal{J}_{ij}/\mathcal{J}_0$.

Thus one obtains the results for the special cases:

$$\begin{array}{lll} J_{12}=1, \quad J_{13}=J_{23}=0 & E^B_0(Z_2+Z)=\mathcal{J}_0 & E^B_1(Z_2+Z)=-\mathcal{J}_0 \\ J_{12}=J_{23}=1, \quad J_{13}=0 & E^B_0(Z_3\ \text{lin})=\mathcal{J}_0 & E^B_1(Z_3\ \text{lin})=-\mathcal{J}_0 \\ J_{12}=J_{13}=J_{23}=1 & E^B_0(Z_3\ \text{cyc})=0 & E^B_1(Z_3\ \text{cyc})=0. \end{array} \tag{8}$$

In this simple HL model Z_2+Z has the same energy as linear Z_3, and for the D_{3h} arrangement, which is higher in energy, the two states are degenerate, but if J_{ij} is assumed to be larger for Z_2+Z than for linear Z_3, the former becomes energetically favoured. The distance dependence of the J_{ij} is rather complicated; we therefore do not take it into account explicitly but evaluate the properties of the system as a function of the J_{ij}.

In order to be able to assess the validity of the HMO and the HL model, also VBCI calculations were performed for H_3, which is the simplest example of a three-electron three-centre problem [17]. The ground state and the first excited state were calculated separately with a minimum basis of 1s STO's approximated as contractions of four GTO's with orbital exponents optimized as well as the centres of the orbitals floated. The results are collected together with literature data for the energy barrier height of the linear and non-linear attack in Table 1 and Table 2. They are very similar to results of Shavitt et al. [4], who used the same kind of basis set, and differ by a factor of 2 from the best results available for a large basis including diffuse functions [5]. This relation is approximately the same for all geometries considered. This as well as the results of

Table 1. Saddle point geometries and activation energies for the H_2+H exchange reaction

	$R_{12}=R_{23}$ [a.u.]	ΔE [kJ/mol]
SSMK[a]	1.883	98
SSMK	1.764	46
Liu[b]	1.757	41
YL[c]	1.742	41
VBCI	1.85	98

[a]SSMK see Ref. [4], [b]Liu see Ref. [5], [c]YL see Ref. [17]

Table 2. Activation energies ΔE [kJ/mol] of nonlinear attack for the H_2+H exchange reaction

	Bond angles			
	180°	150°	120°	90°
SSMK[a]	46	53	77	
YL[b]	41	48	71	117
VBCI	98	107	132	212

[a]SSMK see Ref. [4], [b]YL see Ref. [17]

Norbeck et al. [18] on the reliability of the minimum basis set calculations for the H_3 ground state show, that the accuracy of our results is sufficient for an analysis of the energy hypersurfaces, although especially the bond distances for the saddle point geometries of the reactions are too large and become worse as the bond angle decreases. But the essential features necessary to discuss elementary reactions are given correctly. A detailed comparison of the results for the excited state is not possible, but the general appearance of the potential energy curves discussed below agrees with those given by Zaitsevskii et al. [8].

3. Graphical Presentation

Three internal degrees of freedom Q_1, Q_2, Q_3 specify the geometry of a three-centre problem; they can be chosen for instance as R_{12}, R_{23} and θ. The potential energy hypersurfaces $E(Q_1, Q_2, Q_3)$ are hypersurfaces in a four-dimensional space for which a complete graphical presentation is of course not possible. If the two terminal centres are homonuclear, the system is symmetric with respect to a reflection on every plane including the origin and normal to one of the coordinates Q_1. Thus the presentation of one octant is sufficient to fully describe the system (Fig. 1). Furthermore, if the coordinates chosen as horizontal axes Q_1 and Q_2 are of the same type (e.g. R_{12} and R_{23}), all surfaces of constant Q_3 (e.g. θ) are symmetrical with respect to a reflection on the diagonal $Q_1 = Q_2$, in this case, the energy is fully described by the solid body formed by the surfaces U, D and R in Fig. 1. In Figs. 2–4 the total energy is shown as contour diagram on each of these surfaces, and from the equipotential lines on these surfaces one may estimate the behaviour within the solid body.

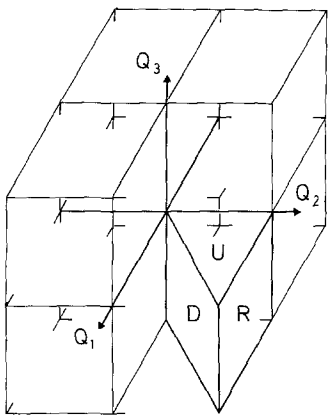

Fig. 1. Complete coordinate space for the three-centre system. The planes which will be used for the graphical representation of the potential hypersurfaces are marked. The labels *U*, *R* and *D* correspond to the upper, the right hand and the diagonal plane, respectively

4. Nonempirical H_3 Calculations

Figure 2 shows the potential energy hypersurfaces of the ground and the first excited doublet state of H_3 with R_{12}, R_{23} and θ as the axes of the solid body representing the potential energy. The upper surface *U* shows one half of the well-known contour diagram of the linear $H+H_2 \rightarrow H_2+H$ reaction, which is symmetrical with respect to the left-hand edge of *U*. *S* is the saddle point, and in Table 1 the calculated parameters of this reaction are collected and compared with the corresponding data from the literature. The right-hand edge of *U* represents the Morse potential with the minimum *M* for the stable H_2 molecule at $R_{12} = 1.4$ a.u. and a distant H atom, and with three isolated H atoms at the front corner *I*. On the right-hand surface *R*, one notices a shallow valley corresponding to a change of θ from 180° to 15°, which leads to a linear arrangement ($\theta = 0°$, not shown in Fig. 2) of H_2 and a distant H atom ($R_{13} = R_{23} - R_{12} = 2.6$ a.u.).

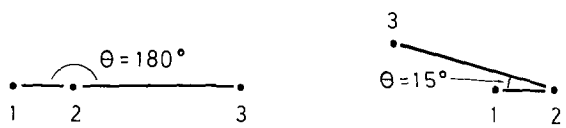

The left-hand surface *D* is characterized by a narrow but steep ridge which crosses it at $\theta = 60°$ corresponding to equilateral triangle geometries, which are, for given bond distances $R_{12} = R_{23}$, the energetically most unfavourable arrangements. Thus, starting from a linear geometry, the energy increases with decreasing valence angle, the increase being less steep if the bond distances are allowed to increase simultaneously. On the other side of the ridge there is a valley which leads to a stable H_2 molecule and a distant H atom in a perpendicular arrangement ($R_{12} = R_{23}$, $\theta \sim 20°$).

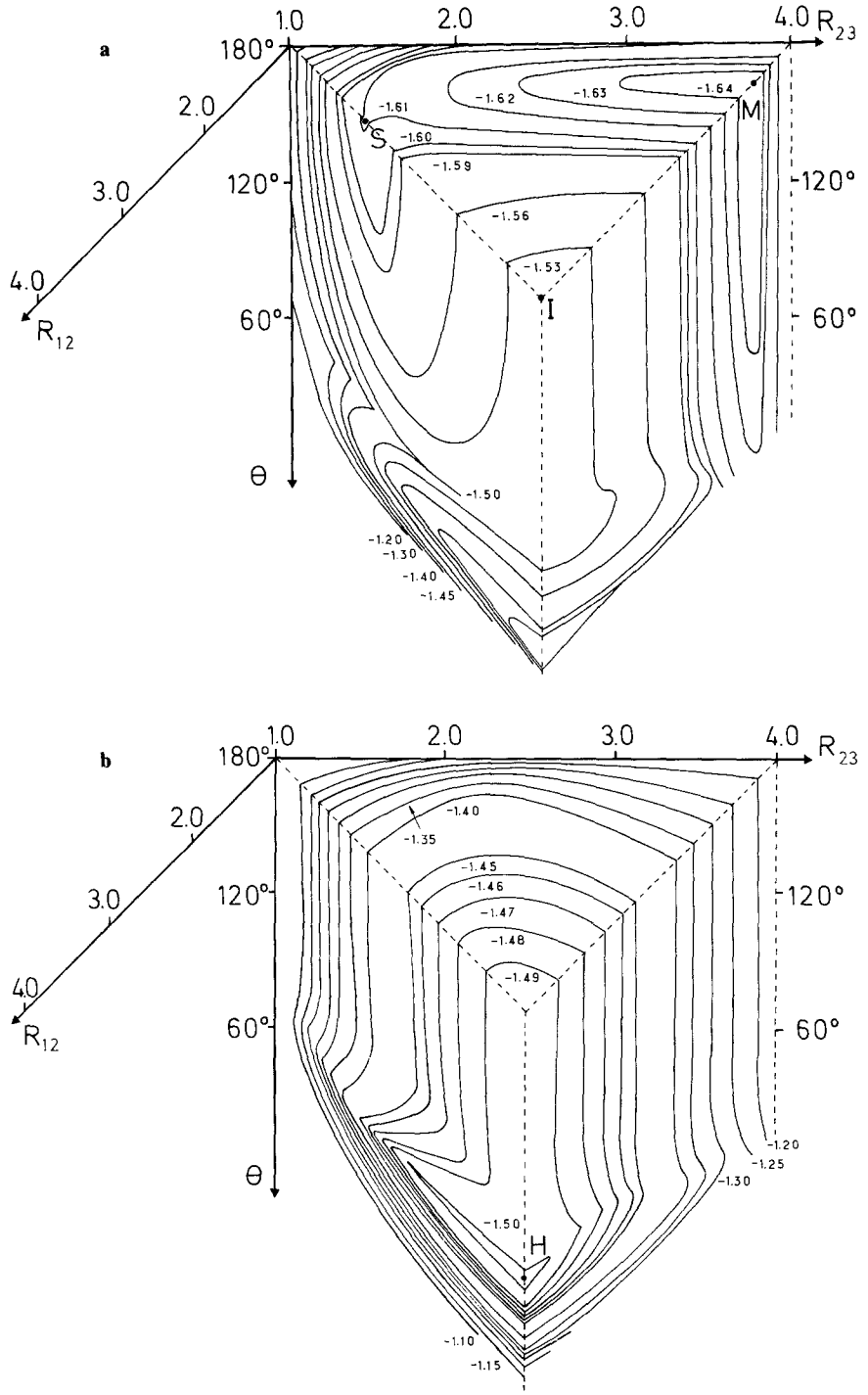

Fig. 2a, b. Potential hypersurfaces for the ground state (**a**) and the lowest excited state (**b**) of the H_3 system calculated by the VBCI method. The energies are given in a.u.

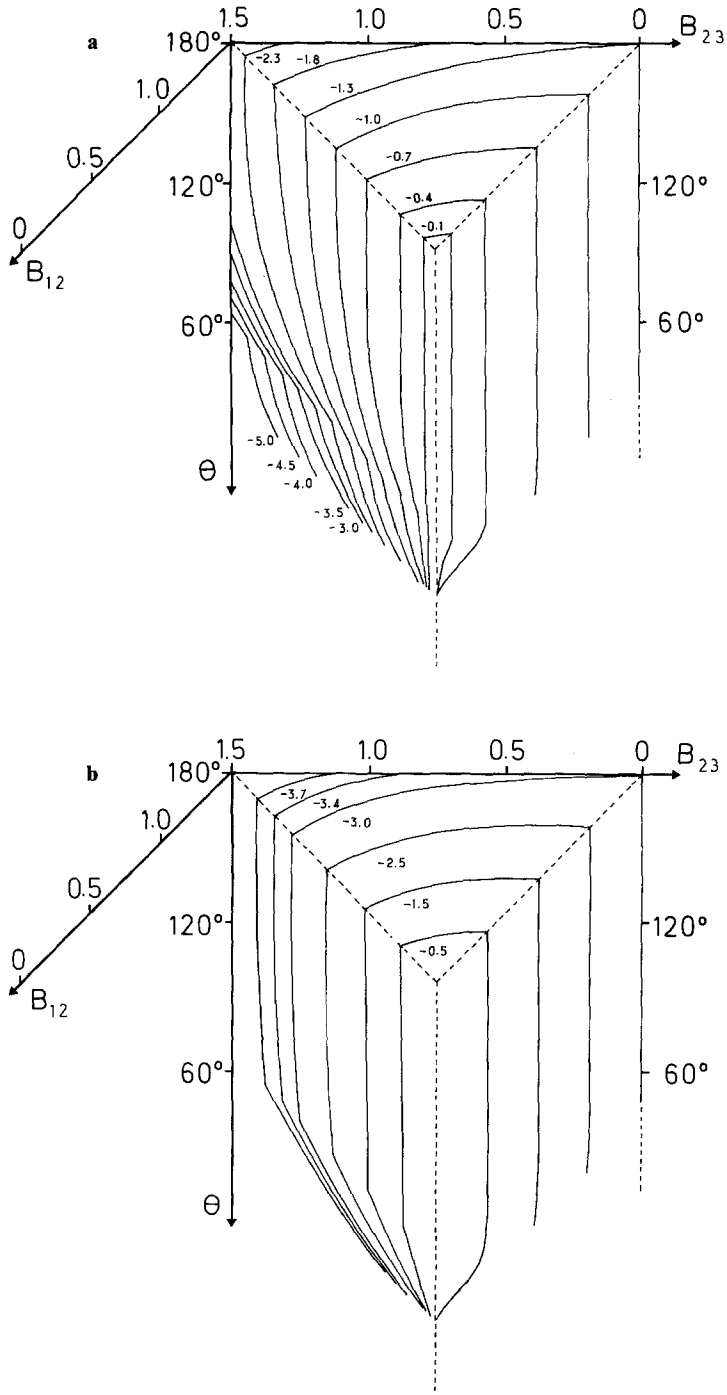

Fig. 3a, b. Potential hypersurfaces for the ground configuration (**a**) and the lowest excited configuration (**b**) of the three-centre three-electron system calculated by the HMO method. The binding energies are given in β_0

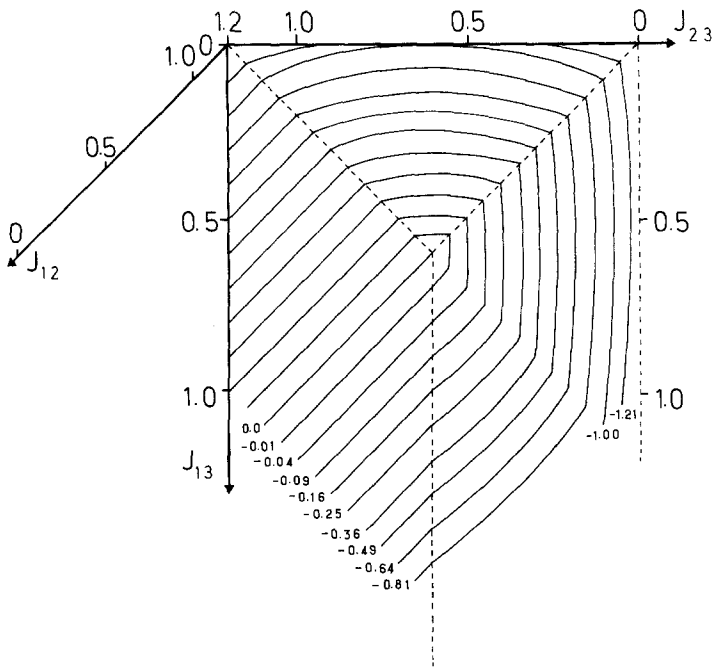

Fig. 4. Potential hypersurfaces for the ground state of the three-centre three-electron system calculated by the HL method. The binding energies are given in $\mathcal{J}_0$

The excited state is characterized on the one hand by a tendency to dissociate into three independent H atoms and by a preference of D_{3h} geometries on the other hand. Thus the upper surface U indicates, that the energy decreases steadily with increasing bond distances, whereas the surfaces D and R show a valley at $\theta = 60°$ which leads to a hole H on the front edge; it represents the energetically most favourable arrangement of the depicted body and corresponds to an equilateral triangle with large bond distances. Due to the stabilization of D_{3h} geometries in the excited state and the destabilization of the same geometries in the ground state, the hypersurfaces of these two states come quite close to each other along this line.

5. HMO Calculations

In Fig. 3 the parameters B_{12}, B_{23} ranging from 1.5 to 0, corresponding to the bond distance in the Z_2+Z system and to infinite separation respectively, and the valence angle θ are used as the three axes for the representation of the potential energy. Thus, the HMO results for the ground and excited state of the three-centre three-electron problem may be easily compared with the VBCI results for H_3 in Fig. 2. In contrast to Fig. 2 the two diagrams of Fig. 3 are very similar; according to the HMO results both the ground state and the excited state tend to collapse into the united atom, the energetically most favourable

point being for both states at the lower rear corner of the body. The main feature of the diagrams is a crack on the surface D at $\theta = 60°$ which corresponds to the ridge and the valley, respectively, on the corresponding VBCI surfaces in Fig. 2. Above this crack, i.e. for valence angles $\theta > 60°$ the energy of the excited state decreases more rapidly with decreasing θ and for constant R_{12} and R_{23} than the ground state energy, as is seen from the larger curvature of the contour lines: below the crack, the ground state surface is steeper. Along the $\theta = 60°$ line the two surfaces touch each other.

6. Empirical HL Calculations

Due to the symmetry of the energy formula Eq. (7) with respect to $E_{0,1}^{B} = 0$, the HL results for the ground and excited state differ only in the sign, so that in Fig. 4 only the ground state potential energy is given. It is plotted as a function of the parameters J_{12}, J_{13} and J_{23}. Thus, the diagram looks rather different from those in Fig. 2 and Fig. 3. The prominent feature of the D_{3h} geometries is no longer a horizontal line but rather the diagonal of the surface D. Both, the most contracted geometry, situated at the lower rear left-hand corner, as well as the upper front corner, corresponding to separated atoms, lie on this line and are therefore energetically unfavourable.

7. Reaction Paths

In this section we shall discuss the following three different reactions: the linear attack, the perpendicular attack and the ring closure reaction.

In Figs. 5–7 sections through the potential energy surfaces are given, which show the reaction diagrams both for the ground and the excited state for all three models considered. Due to the choice of the HMO parameters, the paths for this method are identical to the ones of the VBCI calculations, whereas the reaction paths for the HL method are estimated at characteristic points using for instance $J_{ij} = 1$ and $J_{12} = 1.2$ for the bond in linear Z_3 and $Z_2 + Z$ respectively. The reactions do not follow minimum energy paths for either of the empirical models.

7.1. The Linear Attack

The reaction path for the linear attack leads from point M corresponding to an H_2 molecule and a distant H atom to point S with $D_{\infty h}$ geometry; the bond distance increases during this process from $R_{12} = 1.4$ a.u. to $R_{12} = R_{23} = 1.85$ a.u. For the VBCI ground state this corresponds to the path leading from the minimum for the stable H_2 molecule to the saddle point; Fig. 5a shows the corresponding activation barrier. In the first excited state, the energy decreases without any activation barrier along this path, but S does not correspond to a stable minimum.

The HMO results in Fig. 5b are quite similar for the ground configuration with an energy barrier for the linear attack. In contrast to the VBCI calculations the

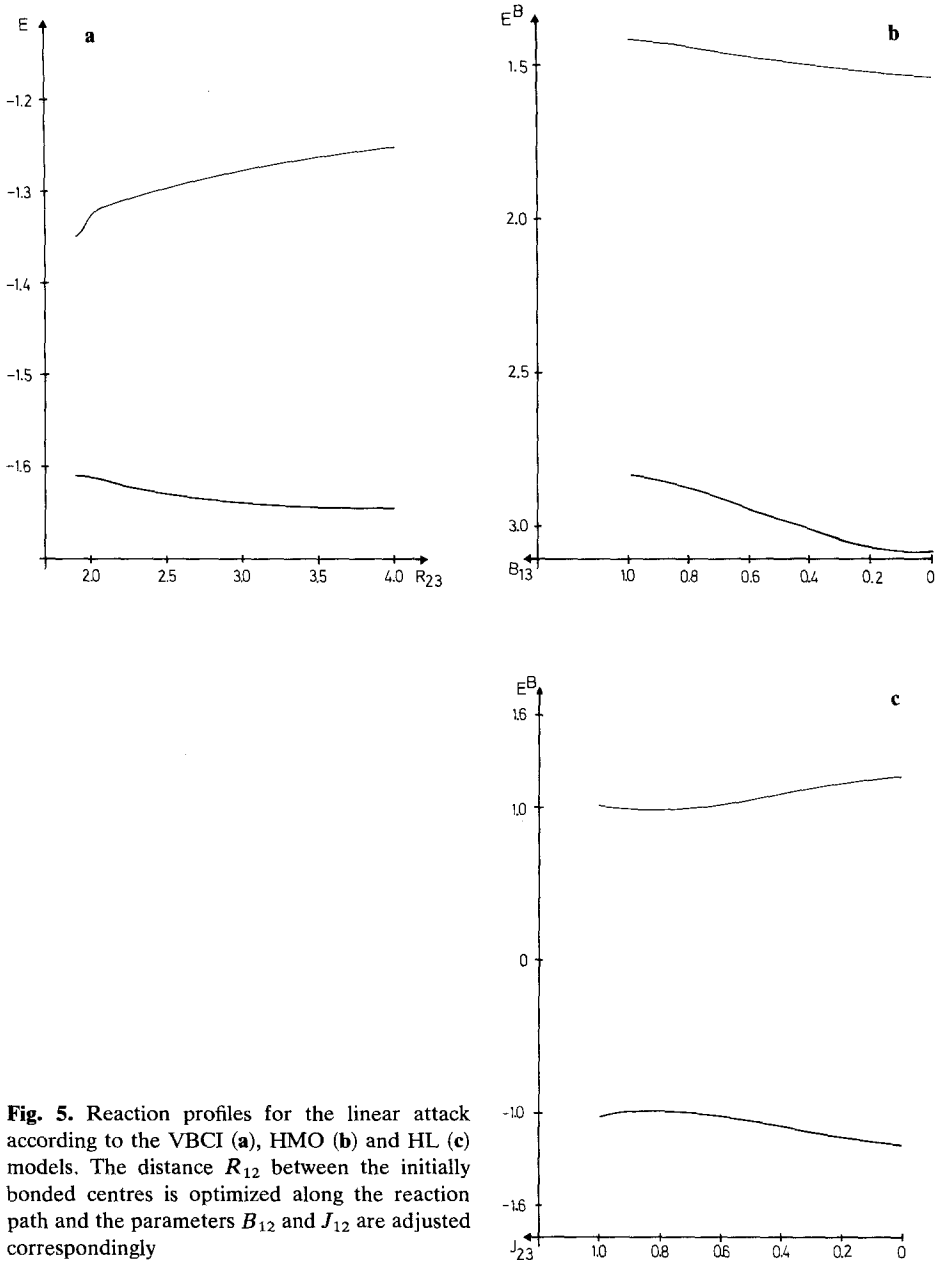

Fig. 5. Reaction profiles for the linear attack according to the VBCI (**a**), HMO (**b**) and HL (**c**) models. The distance R_{12} between the initially bonded centres is optimized along the reaction path and the parameters B_{12} and J_{12} are adjusted correspondingly

potential curve for the first excited configuration increases steadily. The HL results in Fig. 5c are seen to show the correct behaviour for large distances, but at the geometry of the expected transition state the slopes of both curves are just opposite to that obtained from the VBCI calculations.

7.2. The Perpendicular Attack

According to Fig. 2a, b, the perpendicular attack may be described by going on the surface D from the lower front corner ($R_{12} = R_{23} = 4.0$ a.u. and $\theta \sim 20°$, which correspond to $R_{13} = 1.4$ a.u.) over the ridge at $\theta = 60°$, to the point S on the edge between the surfaces D and U. Thus, during the perpendicular attack the bond distance R_{13} increases, and the attacking centre 2 gets finally inserted into the middle of that bond. In Fig. 6 the section through the VBCI surfaces

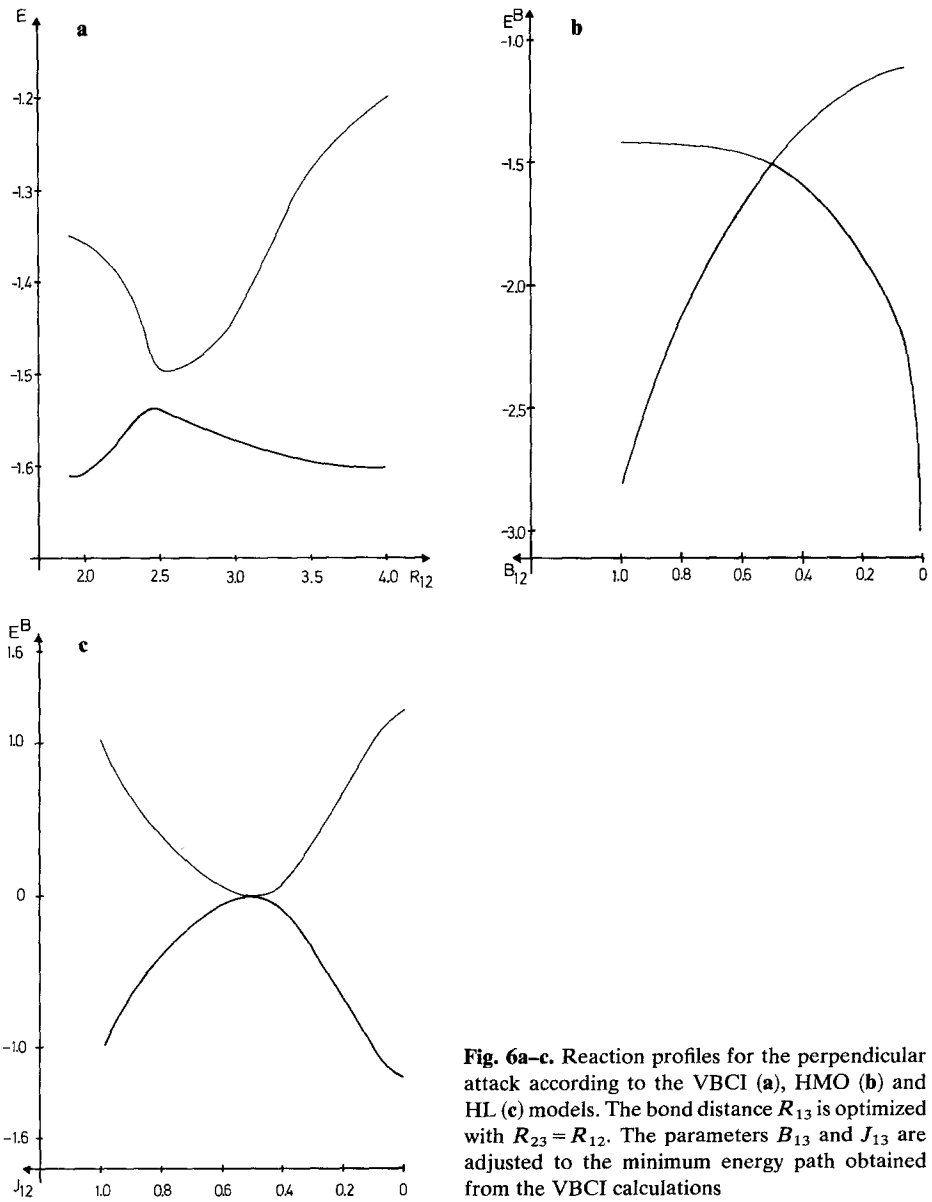

Fig. 6a–c. Reaction profiles for the perpendicular attack according to the VBCI (**a**), HMO (**b**) and HL (**c**) models. The bond distance R_{13} is optimized with $R_{23} = R_{12}$. The parameters B_{13} and J_{13} are adjusted to the minimum energy path obtained from the VBCI calculations

shows that the ground state energy rises to a sharp maximum at the ridge at $\theta = 60°$, where the excited state has a narrow minimum. The HMO model yields a rather similar reaction profile but at the D_{3h} geometries the configurations are degenerate. In the HL model the two crossing hypersurfaces have opposite slopes along the reaction coordinate, so that the D_{3h} geometry, where ground and excited state are degenerate, corresponds to a maximum and a minimum, respectively.

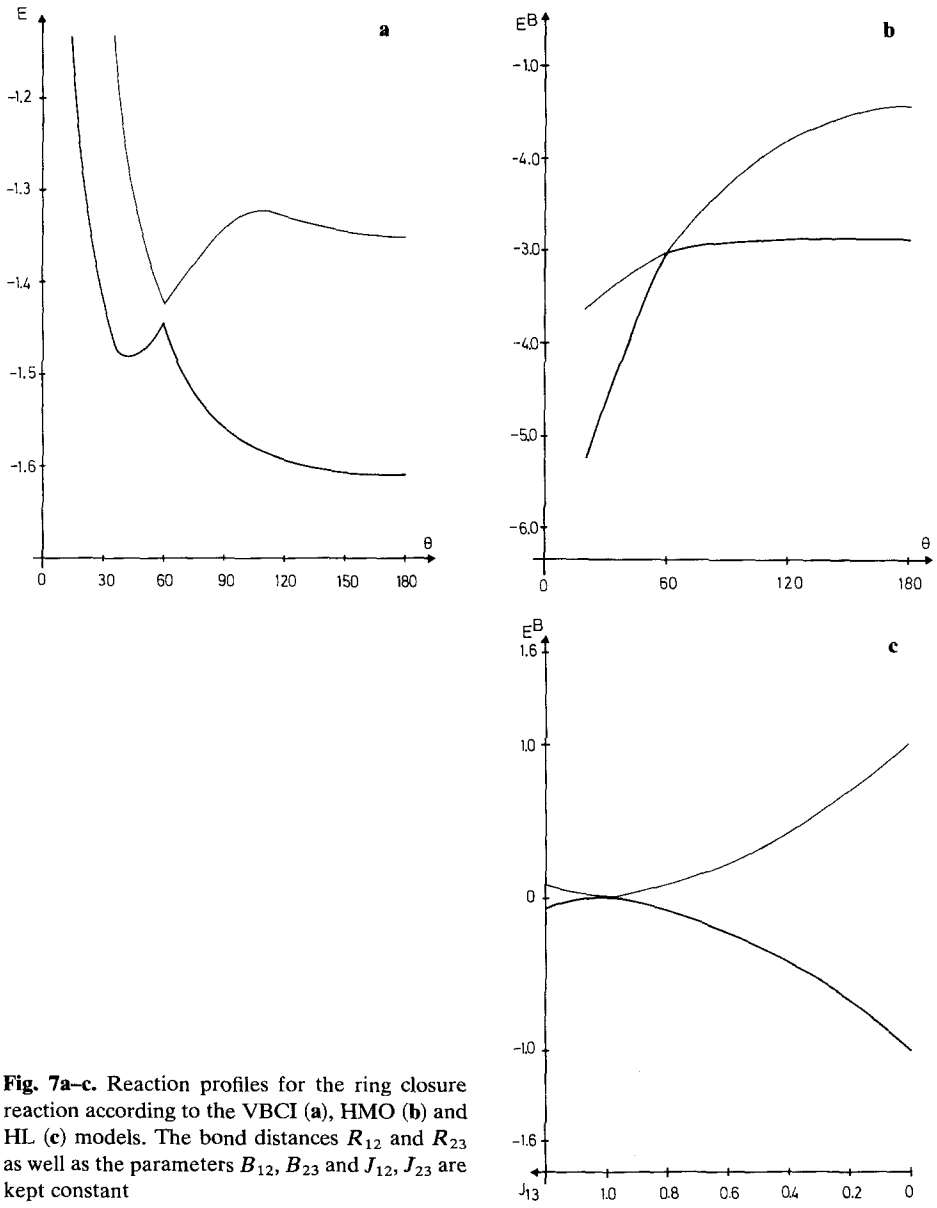

Fig. 7a–c. Reaction profiles for the ring closure reaction according to the VBCI (**a**), HMO (**b**) and HL (**c**) models. The bond distances R_{12} and R_{23} as well as the parameters B_{12}, B_{23} and J_{12}, J_{23} are kept constant

7.3. The Ring Closure Reaction

The reaction path for the ring closure reaction is chosen in a way that only the valence angle θ changes, whereas the bond distances R_{12} and R_{23} are kept equal and constant. It starts at point S and goes down on the surface D parallel to the θ axis. As this path goes over the ridge at $\theta = 60°$ this reaction is also characterized by a surface crossing within the HMO and HL models and the diagrams in Fig. 7 look very much the same as those of the perpendicular attack in Fig. 6. This is particularly true for the HL model, whereas from the VBCI results in Fig. 7a it is seen, that the ground state curve rises again after a minimum at approximately 30°, as is to be expected. The potential curves for this reaction given by the HMO model is rather different to the one for the perpendicular attack. The energy of both configurations decreases and therefore the expected degeneracy at $\theta = 60°$ corresponds to neither a maximum nor a minimum.

It should be pointed out that, according to Fig. 2, the ridge for the D_{3h} geometries obtained from the VBCI calculations can be avoided, if, instead of keeping the bond distances constant, R_{23} is allowed to increase first and then θ is changed, so that the reaction path goes along the surfaces U and R.

8. Discussion

The most characteristic feature of the potential energy surfaces based both on the HMO as well as on the HL model is the degeneracy of the ground state and the lowest excited state for all geometries with equal bond distances, which is a consequence of the D_{3h} symmetry of the system. This phenomenon gives rise to a Jahn–Teller distortion [19, 20].

In both models the system is stabilized if the symmetry is reduced to C_{2v}, but the models predict different types of distortion. If the bond distances R_{12} and R_{23} are kept constant, the HMO model describes the decrease of the bond angle θ corresponding to a shortening of the bond distance R_{13} to be energetically most favourable (Eq. (1) and Fig. 3a), whereas the increase of θ and stretching of R_{13} is favoured in the HL picture (Eq. (5) and Fig. 4a). Or, more generally, it is energetically most favourable for the Z_3 triangle to shrink and to expand according to the HMO model and the HL model, respectively.

The wave functions of the two states considered span the two-dimensional irreducible representation E' of the D_{3h} point group, therefore the degeneracy cannot be lifted by considering only these two states. Eq. (5) shows that the off-diagonal element vanishes if $J_{23} = J_{13}$. This is true as long as the symmetry is at least C_{2v}, in which case the ground and the excited state are described by $^2\Psi_2$ and $^2\Psi_1$, respectively, if the valence angle at centre 2 is smaller than 60°, and vice versa for larger angles. If in the VBCI calculations the orbital exponents are optimized and the orbitals are floated without any symmetry restrictions, wave functions of lower symmetry than D_{3h} are obtained, and therefore the potential surfaces of the ground state and lowest excited state do not cross at equilateral triangle geometries of the nuclear arrangement.

Both, the HMO and the HL method neglect the nucleus–nucleus repulsion, which is assumed to be included in the constants α of the HMO model or A of the HL approach. This assumption is reasonable for normal bond lengths and longer distances, but it breaks down when the atoms start penetrating each other. Thus, both models lead to incorrect results for small distances, although they differ in so far as the geometry shown at the lower rear left hand corner in Figs. 3 and 4 is most favoured in the HMO model, but not favoured in the HL model.

Within the HMO model the perpendicular attack is energetically unfavoured, whereas the ring closure is favoured, as may be seen from Figs. 6b and 7b. For the perpendicular attack all bond distances are longer and therefore the $B_{\mu\nu}$ values are smaller than for the ring closure reaction. As all $B_{\mu\nu}$ enter the energy expression (Eq. (1)) with the same sign, the energy of the ground configuration decreases if any additional bond is formed or if all $B_{\mu\nu}$ increase during a reaction. Thus, the different predictions for the two reactions can be understood.

The parametrization with the β values proportional to overlap integrals is rather sensitive to the peculiarities of the system under investigation and requires either detailed information or judicious estimates in order to obtain reliable results. The description of the linear attack is a good example for this. The HMO result for this reaction depends on the ratio of the $B_{\mu\nu}$ values in the Z_2+Z and the linear Z_3 arrangements; an activation barrier is obtained only if this ratio is larger than 1.4.

Recently Calzaferri [10] pointed out that the inclusion of overlap between all centres makes the linear H_3 unstable with respect to the H_2+H even for non-optimized parameters. This correct ordering of the relative energies is due to the appropriate normalization of the wave functions. Also for linear and cyclic H_3 EHT calculations using the same β values for either geometry lead to the correct energetical ordering.

The HL model predicts for the linear attack a shallow minimum at the point where the transition state is to be expected, because the J_{13} value is kept equal to zero for all arrangements along the reaction path; in spite of this minimum an activation energy is calculated for this reaction, because the energy of the linear geometry is higher than that of the Z_2+Z system. For exact calculations the linear Z_3 arrangement will be shifted slightly below the edge between the U and D surfaces (Fig. 4) and will be of higher energy.

In contrast to the HMO results the HL model *always* gives higher energies for cyclic (D_{3h}) than for linear ($D_{\infty h}$) structures (cf. Eq. (8)). Fig. 4 shows that the activation energy for the cyclization calculated by the parametrized HL model is the same for all values of J_{ij} and that it is impossible to make the perpendicular attack or the ring closure less forbidden. This is due to the fact that the energies depend on the differences of the parameters and therefore any additional bond destabilizes the system (Eq. (7)). Thus, the HL model generally reveals those characteristics of the three-centre three-electron system which show up in the results of the nonempirical VBCI calculations for H_3.

In this connection it seems to be interesting to compare the conclusions from the HMO and the HL models with the results from the Yamaguchi theory of radical reactions [11], which is based on the Heisenberg spin operator. In this approach two doublet spin eigenfunctions are used, and the exchange integral J is taken as a parameter with a distance dependence comparable with that of our J_{ij} parameter. For the linear attack this theory gives results in agreement with the expectation from the other models, but for the perpendicular attack no activation barrier is obtained; the ground state energy is shown to be constant up to the D_{3h} geometry and to decrease beyond this point. If the HMO and HL results for a perpendicular attack are to be compared with this spin operator approach, the parameters B_{13} and J_{13}, respectively, have to be kept constant in order to describe the same reaction path. These restrictions are of minor importance for the HL results, but they change drastically the HMO results in so far as now the energy decreases along the reaction path, for similar reasons as discussed for the ring closure reaction.

From the energy hypersurfaces obtained from non-empirical VBCI calculations, it is seen that any geometry with bond angles smaller than 180° is disadvantageous. Any reaction involving bond angle distortions must therefore pass over an activation barrier, and all reaction paths involving equilateral triangular geometries are forbidden. Thus all intramolecular rearrangement reactions finally lead to the $H_2 + H$ system. The lowest excited doublet state is purely dissociative at every point. The most favourable way to dissociation follows the rather deep but narrow valley along the 60° line.

If the non-empirical H_3 results are to be used to predict the properties of general three-centre three-electron problems or of more complex systems, which in a first approximation may formally be treated as three-centre three-electron problems, the following points should be kept in mind. All those reactions, which start or end at the cyclic $D_{\infty h}$ structure, run along a steep slope or involve arrangements from where it is most favourable to dissociate into the $H_2 + H$ system. Thus the reaction paths for corresponding model reactions have to be chosen more or less arbitrarily. Due to the symmetry of the basis AO's no predictions concerning the influence of the orbital phase can be made. This is important for example if a perpendicular attack on one centre of the initial bond with zero overlap to the other centre is to be discussed. Such a reaction was predicted by Bonačić-Koutecký et al. [12] to be as favourable as the linear approach.

Taking into account the limitations of the H_3 system as a model for more general systems, we come to the following conclusions: Every cyclic arrangement of a three-centre three-electron system is energetically unfavourable in the ground state, or in terms of the Woodward–Hoffmann rules [21], every reaction involving these geometries is thermally forbidden, whereas every linear attack is allowed. For reactions upon the hypersurface of the lowest excited state the opposite is true. Due to the crossing of the hypersurfaces at the D_{3h} geometries there exist a funnel [22], through which the system can return to the ground state surface

and form stable products. Thus, ring closure reactions of radicals are forbidden in the ground state but allowed in the excited state.

9. Conclusion

The results of this paper show, that a representation of the potential hypersurfaces by means of the solid body discussed in Fig. 1 is very well suited not only to study the different reaction paths, but also to discuss the response of the system to a deviation from a preselected reaction path. Thus, this representation enabled us to gain some additional insight into the mechanism and the requirements of the prototype radical reactions. At the same time, the present approach is particularly suited to compare the performance of different models for radical reactions; a consideration of the complete hypersurfaces makes it possible to pinpoint more closely the similarities and differences of the models.

These comparisons show that the simple HL method yields qualitatively reliable results for the Z_3 system, even for the crude parametrization leading to the London formula Eq. (7), which is simple enough to be solved exactly and to be interpreted easily. The disadvantage is, that the method is difficult to extend to heteronuclear systems, as the $\mathcal{J}_{ij}$ terms contain contributions from all centres, so that changes on one of the centres cannot be taken into account.

To understand the failures of the various models, a closer look at the inherent approximations and the wavefunctions is helpful.

If the configurations used in the HMO model are expanded into the AO basis, the following three types of orbital products occur: (1) $\chi_\mu\chi_\mu\chi_\mu$, (2) $\chi_\mu\chi_\mu\chi_\nu$ and (3) $\chi_\mu\chi_\nu\chi_\rho$. Since these products do not fulfil the antisymmetry condition, all of the first type and some of the second type can be called "nonsensical", because the same AO is occupied by at least two electrons with identical quantum numbers. The remaining terms of the second type may be called "ionic" and "covalent", respectively. Within the ZDO approximation the two centre integrals $h_{\mu\nu}$ are only obtained from the interaction of the products of type 1 and 2 respectively. Thus the "covalent" terms do not contribute to the binding energy.

The "nonsensical" terms occur due to the neglect of spin correlation, whereas the Coulomb correlation is dependent on the relative contribution of the remaining "ionic" and the "covalent" terms. In the VB approach the effect of electron correlation can be discussed by considering the contributions of the covalent and the ionic structures, which are given by the sums over the squares of their coefficients in the wavefunction. The portion of the ionic structures is approximately zero for the Z_2+Z system and increases to 0.27 for the linear and to 0.37 for the cyclic Z_3, showing that correlation is least important for the latter arrangement. Hence, it must be concluded that the HMO model describes the Z_2+Z and linear Z_3 geometries worse than the cyclic geometry, and that the HL model overestimates the destabilization due to cyclization.

If overlap is included the two-centre integrals $h_{\mu\nu}$ enter the matrix elements not only as in the HMO model, but also in a general form multiplied by overlap

integrals. Therefore the "covalent" orbital products contribute to the binding energy and the Z_2+Z and linear Z_3 arrangements are described much better leading to the good EHT results [23]. The main effects of the overlap can be included into the parameters β by a judicious choice (cf. Fig. 6).

The Yamaguchi spin functions contain the electron correlation in a way comparable with the HL model, but the restricted inclusion of electron interaction, due to the Heisenberg spin operator, deteriorates the results.

Thus, whereas electron interaction is of crucial importance within the AO methods, it is the overlap which matters in the MO models. Results of *PPP* type calculations, which take into account electron interaction but not overlap, show no significant improvement over the simple HMO model, whereas nonempirical calculations including both yield the correct relative energies for the different arrangements [5]. It is not easy to combine the advantages of the various models in order to design a method, which is simple, fast and easy to interpret.

Many molecular systems that can be reduced to a Z_3 system, as for instance the attack of a methyl radical on ethylene or H_2 and the intramolecular rearrangement of the allyl system, have been the subject of experimental as well as theoretical investigations [24]. The results can be understood on the basis of those features of the radical reactions which in the discussion above were shown to be essential, in spite of geometrical constraints such as σ bonds between reacting sites or the complexity of the substrates. Especially, the Baldwin rules [25] for the intramolecular cyclization of radicals, that were derived experimentally, can be justified theoretically on the basis of our results.

Finally, we should like to mention that the results given in the present paper are pertinent not only to the H_3 problem and the radical reactions discussed above. The investigations on larger radical systems with an odd number of centres should be based on the Z_3 results, because the larger systems can be divided up into Z_3 subunits and the remaining centres can be looked at as a perturbation to these.

Acknowledgement. We thank R. D. Poshusta for making the program PGAUSS available to us.

References

1. Truhlar, D. G., Wyatt, R. E.: Ann. Rev. Phys. Chem. **27**, 1 (1976); Truhlar, D. G., Wyatt, R. E.: Adv. Chem. Phys. **36**, 141 (1977); Dabrowski, I. Herzberg, G.: Can. J. Phys. **58**, 1238 (1980); Porter, R. N.: Ber. Bunsenges. Phys. Chem. **86**, 407 (1982)
2. King, H. F., Morokuma, K.: J. Chem. Phys. **71**, 3213 (1979); Jungen, M.: J. Chem. Phys. **71**, 3540 (1979); Martin, R. L.: J. Chem. Phys. **71**, 3541 (1979)
3. Herzberg, G.: J. Chem. Phys. **70**, 4806 (1979)
4. Shavitt, I., Stevens, R. M., Minn, F. L., Karplus, M.: J. Chem. Phys. **48**, 2700 (1968)
5. Liu, B.: J. Chem. Phys. **58**, 1925 (1973); Siegbahn, P., Liu, B.: J. Chem. Phys. **68**, 2457 (1978)
6. Truhlar, D. G., Horowitz, C. J.: J. Chem. Phys. **68**, 2466 (1978)
7. Tennyson, J.: Chem. Phys. Lett. **86**, 181 (1982)

8. Zaitsevskii, A. V., Nemukhin, A. V., Stepanov, N. F.: Mol. Phys. **41**, 377 (1980)
9. Wu, A. A., Mol. Phys. **42**, 379 (1981)
10. Calzaferri, G.: Chem. Phys. Letters **87**, 443 (1982)
11. Yamaguchi, K.: Chem. Phys. Letters **28**, 93 (1974); Yamaguchi, K., Fueno, T.: Chem. Phys. Letters **38**, 51 (1976)
12. Bonaćić-Koutecký, V., Koutecký, J., Salem, L.: J. Am. Chem. Soc. **99**, 842 (1977).
13. Gerhartz, W., Poshusta, R. D., Michl, J.: J. Am. Chem. Soc. **98**, 6427 (1976).
14. Matsen, F. A.: Acc. Chem. Res. **11**, 387 (1978)
15. Epiotis, N. D.: Unified valence bond theory of electronic structure. Berlin, Heidelberg, New York: Springer-Verlag 1982
16. London, F.: Z. Elektrochem. **35**, 552 (1929)
17. Yates, A. C., Lester Jr., W. A.: Chem. Phys. Letters **24**, 305 (1974)
18. Norbeck, J. M., Certain, P. R., Tang, K. T.: J. Chem. Phys. **63**, 590 (1975); Norbeck, J. M., Certain, P. R.: J. Chem. Phys. **63**, 4127 (1975)
19. Jahn, H. A., Teller, E.: Proc. Roy. Soc. (London) **A161**, 220 (1937)
20. Porter, R. N., Stevens, R. M., Karplus, M.: J. Chem. Phys. **49**, 11 (1968)
21. Woodward, R. B., Hoffmann, R.: J. Am. Chem. Soc. **87**, 395 (1965)
22. Michl, J.: Mol. Photochem. **4**, 243 (1972); Michl, J.: Mol. Photochem. **4**, 257 (1972)
23. Malcolme-Lawes, D. J.: J. Chem. Soc. Faraday Trans. II. **71**, 1183 (1975)
24. Poutsma, M. L.: Free radicals, Vol. 2, p. 63, edited by Kochi, J. K. New York: Wiley 1973; Dewar, M. J. S., Olivella, S.: J. Am. Chem. Soc. **100**, 5290 (1978); Nagase, S., Kern, C. W.: J. Am. Chem. Soc. **102**, 4513 (1980)
25. Baldwin, J. E.: J. C. S. Chem. Comm. 736 (1976)

Received February 21, 1983